Available online at www.sciencedirect.com
ScienceDirect
Physics Letters A 372 (2008) 3109–3117
PHYSICS LETTERS A
www.elsevier.com/locate/pla

Two-photon spectral coherence matrix and characterization of multi-parameter entangled states

C. Bonato [a,b,*], P. Villoresi [b], A.V. Sergienko [a]

[a] *Quantum Imaging Laboratory, Department of Electrical and Computer Engineering, Boston University, Boston, MA, USA*
[b] *CNR-INFM LUXOR, Department of Information Engineering, University of Padova, Padova, Italy*

Received 11 December 2007; received in revised form 29 December 2007; accepted 4 January 2008

Available online 15 January 2008

Communicated by P.R. Holland

Abstract

In this Letter we discuss how the classical coherence matrix can be generalized to describe the quantum properties of broadband two-photon entangled states. Procedures for experimental evaluation of two-photon matrix elements have been outlined. We illustrate how this formalism can be used for characterization of multi-parameter optical entanglement and discuss its possible applications in quantum optical measurement and quantum coherent control.

PACS: 42.50.-p; 42.50.Dv

Keywords: Quantum optics; Entangled photons; Coherence; Polarization

1. Introduction

Quantum entanglement has become a valuable resource in many areas of quantum optics and quantum information processing. In particular, polarization entanglement has contributed to the success of quantum cryptography [1] and enabled some initial demonstrations of elements of quantum information processing such as quantum gates, entanglement swapping, and quantum teleportation [2–4].

Frequency entanglement has manifested itself in the quantum dispersion cancellation effect [5,6] that has been demonstrated with frequency-anticorrelated states, and has found several applications in the area of precise optical measurement [7,8]. The use of frequency-entangled states also promises enhancing the accuracy of clock synchronization and positioning with respect to their classical counterparts [9,10].

Traditionally, states entangled in polarization and frequency have been produced using the nonlinear process of spontaneous parametric down-conversion (SPDC). The physical nature of phase matching during the parametric interaction in birefringent nonlinear crystals leads to a unique interconnection between polarization, frequency, and direction (k-vector) parameters of the electromagnetic field. This results in generation of quantum states that are simultaneously entangled in all of those quantum variables. In many cases, the multi-parameter entangled nature of two-photon states from SPDC has been considered as an unnecessary complication. Very often, researchers constrain the direction of propagation with small pinholes and limit the frequencies of light with narrowband spectral filters in order to encode quantum information on the polarization degree of freedom. However, it has been recognized recently [11,12] that the complexity of multi-parameter polarization-frequency and k-vector entanglement carries significant potential for augmenting resources of quantum information processing.

* Corresponding author.
E-mail address: bonatocr@dei.unipd.it (C. Bonato).

0375-9601/$ – see front matter
doi:10.1016/j.physleta.2008.01.016

The polarization state tomography technique, leading to polarization density matrix reconstruction, has been developed by Kwiat and co-workers in order to provide quantitative characterization of polarization entanglement created in the SPDC [13]. The conventional Stokes parameters formalism of polarization optics has also been extended to cover the domain of two-photon polarization entangled states [14]. In the field of ellipsometry, the reconstruction of the polarization state of light, after reflection from a material, can provide an information about the surface geometry and the chemical composition of the system under investigation. A quantum analog of ellipsometry that makes use of polarization-entangled states has been developed recently [15,16] that provides higher measurement accuracy in the low-power regime [17]. In quantum ellipsometry the retrieval of the two-photon polarization density matrix by using polarization state tomography can provide more accurate characterization of the sample properties even when the source emits polarization entangled light in a mixed state [18].

However, the monochromatic (single-frequency) ellipsometry cannot provide enough information to completely characterize the sample in many challenging applications. This becomes particularly clear when dealing with complex surface geometries, or with layers of materials that have similar refractive indices at the particular probing wavelength. To address this problem, a technique known as spectroscopic ellipsometry has been developed based on polarization properties of spectrally broadband light. Classical spectroscopic ellipsometry is currently used in several areas of nanotechnological metrology [19].

Traditionally, the polarization state of broadband light has been described in terms of the spectral coherence matrix and spectral Stokes parameters [20,21]. In this Letter we introduce the two-photon spectral coherence matrix and the spectral two-photon Stokes parameters along with procedures for evaluating their components in experiment. These tools will be crucial for characterizing multi-parameter entanglement and for developing a quantum version of spectroscopic ellipsometry that is built around spectral and polarization entanglement.

This formalism could also be useful in the description of general nonlinear optical interactions that do not necessarily involve states of fixed polarization. For example, a spectral polarization engineering technique has found an important application in the field of optical attosecond physics. The polarization-gating of spectral components of the original laser pulse allows researchers implementing an efficient control of high-order harmonic generation in order to obtain a single attosecond laser pulse [22–24].

Characterization and control of spectral polarization [25–27] is also important in nonlinear spectroscopy, in photochemistry and in quantum control where ultrashort pulses with carefully designed spectral polarization are employed to drive specific tasks (chemical reactions, molecular alignment, etc.). It was recognized recently that the down-conversion light, even if not coherent, can behave like ultrashort pulses due to its inherent correlation between signal and idler photons. For example, two-photon absorption using down-converted light with spectrally-engineered entangled photons has been demonstrated recently [28]. Our formalism could help in extending these results into areas where spectral polarization is important.

We first briefly review the concepts of spectral coherence matrix and spectral Stokes parameters in classical optics. We then introduce a two-photon spectral coherence matrix and spectral two-photon Stokes parameters for entangled-photon states. In conclusion we outline experimental procedures for evaluation of matrix elements and discuss several special cases.

2. Classical coherence matrix

Classical partially polarized light can be described by the coherence matrix [29]:

$$J(\tau) = \begin{bmatrix} \langle E_H^*(t)E_H(t+\tau)\rangle & \langle E_H^*(t)E_V(t+\tau)\rangle \\ \langle E_V^*(t)E_H(t+\tau)\rangle & \langle E_V^*(t)E_V(t+\tau)\rangle \end{bmatrix} \tag{1}$$

where:

$$\left\langle E_i^*(t)E_j(t+\tau)\right\rangle = \int E_i^*(t)E_j(t+\tau)\,dt \tag{2}$$

or by the spectral coherence matrix [30,31]:

$$R(\omega) = \begin{bmatrix} R_{HH}(\omega) & R_{HV}(\omega) \\ R_{VH}(\omega) & R_{VV}(\omega) \end{bmatrix} \tag{3}$$

where:

$$R_{ij}(\omega) = \int_{-\infty}^{+\infty} J_{ij}(\tau)e^{j\omega\tau}\,d\tau. \tag{4}$$

Since the spectral coherence matrix is Hermitian we can express it in terms of Pauli matrices σ_i, so that:

$$R(\omega) = \frac{1}{2}\sum_{i=0}^{3} S_i(\omega)\sigma_i \tag{5}$$

where the $S_j(\omega)$ are called the spectral Stokes parameters:

$$S_j(\omega) = \mathrm{Tr}\big[\sigma_j R(\omega)\big]. \tag{6}$$

The spectral coherence matrix can be written as:

$$R(\omega) = \frac{1}{2}\begin{bmatrix} S_0(\omega) + S_1(\omega) & S_2(\omega) + iS_3(\omega) \\ S_2(\omega) - iS_3(\omega) & S_0(\omega) - S_1(\omega) \end{bmatrix}. \tag{7}$$

The trace of the spectral coherence matrix equals the spectral intensity:

$$\mathrm{Tr}\big[R(\omega)\big] = R_{HH}(\omega) + R_{VV}(\omega) = S_0(\omega) = I(\omega). \tag{8}$$

If we consider, for example, light described by the Jones vector:

$$\begin{bmatrix} E_H(t) \\ E_V(t) \end{bmatrix} \tag{9}$$

where:

$$E_i(t) = \int_{-\infty}^{+\infty} \epsilon_i(\omega) e^{-j\omega t}\, d\omega, \tag{10}$$

the elements of the spectral coherence matrix are:

$$R_{ij}(\omega) = \int_{-\infty}^{+\infty} \big\langle E_i(t) E_j^*(t+\tau)\big\rangle e^{j\omega\tau}\, d\omega \tag{11}$$

$$= \epsilon_i(\omega)\epsilon_j^*(\omega). \tag{12}$$

Therefore:

$$R(\omega) = \begin{bmatrix} |\epsilon_H(\omega)|^2 & \epsilon_H^*(\omega)\epsilon_V(\omega) \\ \epsilon_H(\omega)\epsilon_V^*(\omega) & |\epsilon_V(\omega)|^2 \end{bmatrix}. \tag{13}$$

Stokes parameters cannot be generally defined for the coherence matrix since it is Hermitian only for $\tau = 0$:

$$J^\dagger(\tau) = J(-\tau). \tag{14}$$

3. Two-photon case

Consider the setup in Fig. 1. The two separate spatial modes are projected by two identical tomography devices and coincidence events between the two arms are detected. Each tomography device consists of a polarization tomography part followed by a Michelson interferometer in collinear configuration. It is preferable to use an interferometric configuration for evaluation of spectral properties with respect to one based on a monochromator. In Fourier-transform interferometry spectral resolution can be made arbitrarily high by increasing the measurement interval, and, due to multiplex advantage [32], a higher signal-to-noise ratio is attainable in the case of the additive noise, that is common in single-photon measurements [33].

The polarization tomography device [13] converts the information regarding the polarization state into the amplitude of a linear polarized state. It consists of a quarter-wave plate (at angle q with respect to the vertical direction), a half-wave plate (at angle h) and a vertical linear polarizer, described by the Jones matrix:

$$T(h,q) = T_{\mathrm{POL}}(\theta = 0) T_{\lambda/2}(h) T_{\lambda/4}(q) = \frac{1}{2\sqrt{2}}\begin{bmatrix} 0 & 0 \\ 0 & 1 \end{bmatrix}\begin{bmatrix} \cos 2h & \sin 2h \\ \sin 2h & -\cos 2h \end{bmatrix}\begin{bmatrix} i - \cos 2q & \sin 2q \\ \sin 2q & i + \cos 2q \end{bmatrix}$$

$$= \begin{bmatrix} 0 & 0 \\ \zeta_1(h,q) & \zeta_2(h,q) \end{bmatrix}.$$

In the collinear Michelson interferometer the input vertically polarized light is first rotated by 45 degrees thus providing equal horizontal and vertical projections. Then delay τ between the horizontally-polarized component and the vertically-polarized one is introduced through a birefringent delay-line, comprising two sliding quartz wedges. Finally, both polarization components are recombined again by means of a half-wave plate and a polarizer.

The quantized fields at the detectors are:

$$E_n^{(+)}(t_n) = \sum_{\gamma=0}^{1} \zeta_{n,\gamma} \int d\omega \left(1 + e^{j\omega\tau_n}\right) \hat{a}_{n,\gamma}(\omega) e^{-j\omega t_n} \tag{15}$$

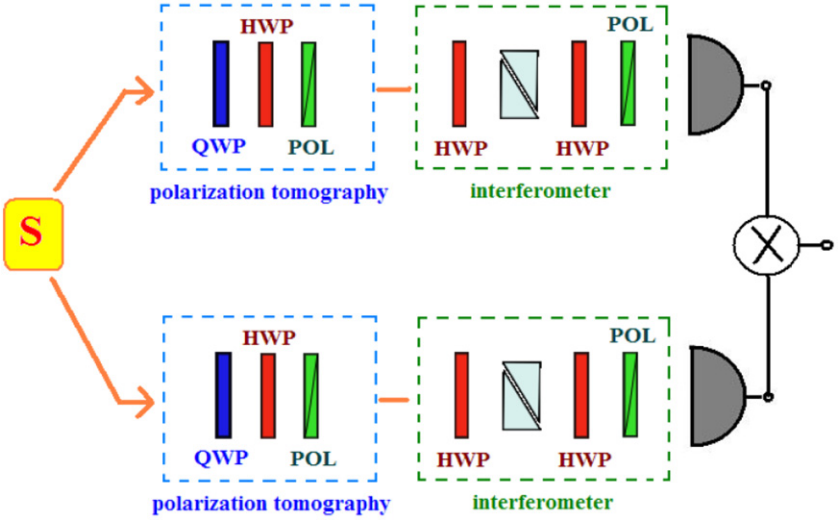

Fig. 1. Schematic of experimental apparatus to measure the two-photon spectral coherence matrix (HWP = half-wave plate, QWP = quarter-wave plate, POL = polarizer). In each of the two separate photon paths there is a tomography device comprising a polarization tomography part and a collinear Michelson interferometer. Scanning 16 independent polarization settings and the two delay-lines one can retrieve the two-photon spectral coherence matrix elements.

with:

$$\zeta_{n,0}(h_n, q_n) = \frac{1}{\sqrt{2}}\{\sin(2h_n) - i\sin[2(h_n - q_n)]\} \tag{16}$$

and:

$$\zeta_{n,1}(h_n, q_n) = -\frac{1}{\sqrt{2}}\{\cos(2h_n) + i\cos[2(h_n - q_n)]\}. \tag{17}$$

3.1. Interferograms

For a two-photon system considering the frequency and polarization degrees of freedom, the density matrix can be written as:

$$\rho = \sum_{i,j,k,l=0}^{1} \int d\Omega \int d\Omega' \int d\Omega'' \int d\Omega''' \rho_{(2i+j),(2k+l)}(\Omega, \Omega', \Omega'', \Omega''') \big|(\Omega, i)_1; (\Omega', j)_2\big\rangle\big\langle(\Omega'', k)_1; (\Omega''', l)_2\big|. \tag{18}$$

The coincidence count rate, integrating over time due to the slow detectors, can be calculated:

$$\begin{aligned} G(\tau_A, \tau_B) &= \int dt_1 \int dt_2 \,\mathrm{Tr}\big[\rho E_1^{(-)}(t_1) E_2^{(-)}(t_2) E_2^{(+)}(t_2) E_1^{(+)}(t_1)\big] \\ &= \sum_{\lambda,\mu,\gamma,\delta=0}^{1} \int d\omega \int d\omega' \,(1 + \cos\omega\tau_A)(1 + \cos\omega'\tau_B)\zeta_\gamma \zeta_\delta \zeta_\lambda^* \zeta_\mu^* \rho_{(2\gamma+\delta),(2\lambda+\mu)}(\omega, \omega'; \omega, \omega'). \end{aligned} \tag{19}$$

Replacing the four one-photon polarization indices ($\gamma, \delta, \lambda, \mu = H, V$) with two two-photon polarization indices:

$$k = 2\gamma + \delta, \quad l = 2\lambda + \mu, \quad k, l = 0, \ldots, 3 \quad (HH,\ HV,\ VH,\ VV) \tag{20}$$

and:

$$B_k = \zeta_\gamma \zeta_\delta, \qquad B_l = \zeta_\lambda \zeta_\mu. \tag{21}$$

So, going back to the coincidence count rate:

$$G(\tau_A, \tau_B) = \sum_{k,l=0}^{3} B_k B_l^* G_{k,l}(\tau_A, \tau_B) \tag{22}$$

where:

$$G_{k,l}(\tau_A, \tau_B) = \int d\omega \int d\omega' \,\rho_{k,l}(\omega, \omega')\big[1 + \cos(\omega\tau_A)\big]\big[1 + \cos(\omega\tau_B)\big]. \tag{23}$$

The interferograms depend on:

$$R_{ij}^{(2)}(\Omega,\Omega') = \rho_{ij}(\Omega,\Omega',\Omega'',\Omega''')|_{\Omega''=\Omega,\,\Omega'''=\Omega'} \tag{24}$$

which we define as the elements of the two-photon spectral coherence matrix.

Since there are 16 unknown functions $R_{ij}^{(2)}$, 16 different polarization measurements (described by the index $\nu = 1,\ldots,16$) are needed, with 16 independent values for $(h_1, q_1; h_2, q_2)$. Let us indicate the measured interferograms with:

$$G^{(\nu)}(\tau_A,\tau_B) = \sum_{k,l=0}^{3} B_l^{(\nu)*} B_k^{(\nu)} G_{kl}(\tau_A,\tau_B). \tag{25}$$

3.2. Two-photon spectral coherence matrix

Let us now introduce the 2D Fourier transform of the interferograms. The calculations are identical to the ones performed for the single-photon case:

$$\begin{aligned} G^{(\nu)}(\Omega,\Omega') &= \int\int G^{(\nu)}(\tau_A,\tau_B) e^{-j\Omega\tau_A} e^{-j\Omega'\tau_B}\, d\tau_A\, d\tau_B \\ &= 2\sum_{k,l=0}^{3} B_l^{(\nu)*} B_k^{(\nu)} \int d\tau_A \int d\tau_B \int d\omega \int d\omega'\, \rho_{kl}(\omega,\omega';\omega,\omega')(1+\cos\omega\tau_A)(1+\cos\omega'\tau_B) e^{-j\Omega\tau_A} e^{-j\Omega'\tau_B}. \end{aligned} \tag{26}$$

This time the physically significant function ($\Omega \geqslant 0$, $\Omega' \geqslant 0$) will be repeated in reversed form in the other three quadrants of the (Ω,Ω') plane. Switching from positive variables to variables defined on the whole real range, and selecting $\Omega > 0$, $\Omega' > 0$ we obtain:

$$G^{(\nu)}(\Omega,\Omega') = \sum_{k,l=0}^{3} B_l^{(\nu)*} B_k^{(\nu)} R_{kl}^{(2)}(\Omega,\Omega'). \tag{27}$$

Introducing the new index: $\mu = 4k + l$, $\mu = 0,\ldots,15$, we can then build the 4-by-4 matrix:

$$\Gamma_{\nu\mu} = B_l^{(\nu)*} B_k^{(\nu)}. \tag{28}$$

We have:

$$G^{(\nu)}(\Omega,\Omega') = \sum_{\mu=0}^{15} \Gamma_{\nu,\mu} \tilde{R}_{\mu}^{(2)}(\Omega,\Omega'). \tag{29}$$

In matrix form:

$$\mathbf{G}(\Omega,\Omega') = \Gamma \tilde{\mathbf{R}}^{(2)}(\Omega,\Omega'). \tag{30}$$

If the tomography apparatus settings have been chosen so that $\det\Gamma \neq 0$:

$$\tilde{\mathbf{R}}^{(2)}(\Omega,\Omega') = \Gamma^{-1}\mathbf{G}(\Omega,\Omega'). \tag{31}$$

The spectral coherence matrix can be obtained with a simple rearrangement of the elements of the vector $\tilde{\mathbf{R}}^{(2)}(\Omega,\Omega')$:

$$\tilde{\mathbf{R}}_{kl}^{(2)} = \mathbf{R}_{4k+l}^{(2)}. \tag{32}$$

3.3. Two-photon spectral Stokes parameters

As in the case of monochromatic twin-photon states, we can now formally express $R^{(2)}(\omega,\omega')$ in terms of the two-photon Pauli matrices $\sigma_{ij} = \sigma_i \otimes \sigma_j$, so that:

$$R^{(2)}(\omega,\omega') = \frac{1}{4}\sum_{i,j=0}^{3} S_{ij}(\omega,\omega')\sigma_{ij}(\omega). \tag{33}$$

The $S_{ij}(\omega,\omega')$ are the spectral two-photon Stokes parameters, generalization of the two-photon Stokes parameters defined by Abouraddy et al. [14]:

$$S_{ij}(\omega,\omega') = \mathrm{Tr}\big[R^{(2)}(\omega,\omega')\sigma_{ij}\big]. \tag{34}$$

4. Examples

4.1. Pure state with general frequency correlation

Consider the state:

$$|\psi\rangle = \int d\omega \int d\omega' \, \Phi(\omega,\omega')\big[\hat{a}^{\dagger}_{1H}(\omega)\hat{a}^{\dagger}_{2V}(\omega') + \hat{a}^{\dagger}_{1V}(\omega')\hat{a}^{\dagger}_{2H}(\omega)\big]|0\rangle \tag{35}$$

where the function $\Phi(\omega,\omega')$ also contains information about the correlations between the frequencies of the two photons. An example could be Gaussian anticorrelation, like:

$$\Phi(\omega,\omega') = e^{-(\omega+\omega'-\Omega_p)^2/\sigma^2}\,\mathrm{sinc}(\Delta\omega). \tag{36}$$

The two-photon wavefunction is given by:

$$\begin{aligned} A(t_1,t_2) &= \langle 0|\hat{E}^{(+)}_2(t_2)\hat{E}^{(+)}_1(t_1)|\psi\rangle \\ &= \frac{1}{4}\int d\omega \int d\omega' \big(1+e^{j\omega\tau_A}\big)\big(1+e^{j\omega\tau_B}\big)e^{-j\omega t_1}e^{-j\omega' t_2}\big\{\zeta_{1H}\zeta_{2V}\Phi(\omega,\omega') + \zeta_{1V}\zeta_{2V}\Phi(\omega',\omega)\big\} \end{aligned} \tag{37}$$

which gives the following bidimensional interferogram:

$$\begin{aligned} G(\tau_A,\tau_B) &= \int dt_1 \int dt_2 \,\big|A(t_1,t_2)\big|^2 \\ &= \frac{1}{4}\int d\omega \int d\omega' \,(1+\cos\omega\tau_A)(1+\cos\omega\tau_B)\big\{|\zeta_{1H}|^2|\zeta_{2V}|^2\big|\Phi(\omega,\omega')\big|^2 + |\zeta_{1V}|^2|\zeta_{2V}|^2\big|\Phi(\omega',\omega)\big|^2 \\ &\quad + \zeta^*_{1H}\zeta^*_{2V}\zeta_{1V}\zeta_{2H}\Phi^*(\omega,\omega')\Phi(\omega',\omega) + \zeta^*_{1V}\zeta^*_{2H}\zeta_{1H}\zeta_{2V}\Phi^*(\omega',\omega)\Phi(\omega,\omega')\big\}. \end{aligned} \tag{38}$$

From this we can extract the matrix:

$$R^{(2)}(\omega,\omega') = \begin{bmatrix} 0 & 0 & 0 & 0 \\ 0 & |\Phi(\omega,\omega')|^2 & \Phi^*(\omega,\omega')\Phi(\omega',\omega) & 0 \\ 0 & \Phi^*(\omega',\omega)\Phi(\omega',\omega) & |\Phi(\omega,\omega')|^2 & 0 \\ 0 & 0 & 0 & 0 \end{bmatrix}. \tag{39}$$

4.2. Frequency-anticorrelated states

States produced by spontaneous parametric down-conversion exhibit frequency anticorrelation as a consequence of energy conservation in the nonlinear process which leads to pair emission. In this specific case, one photon is at frequency ω and the other at frequency $\omega_p - \omega$. The general density matrix is, therefore:

$$\rho = \sum_{i,j,k,l=0}^{1} \int d\Omega \int d\Omega' \, \rho_{(2i+j),(2k+l)}(\Omega,\Omega_p-\Omega,\Omega',\Omega_p-\Omega')\big|(\Omega,i)_1;(\Omega_p-\Omega,j)_2\big\rangle\big\langle(\Omega',k)_1;(\Omega_p-\Omega',l)_2\big|. \tag{40}$$

Due to presence of correlations between the two photons, only one interferometer is needed, so that we have the interferogram:

$$G(\tau_A,0) = 4\sum_{\lambda,\mu,\gamma,\delta=0}^{1}\int d\omega\,(1+\cos\omega\tau_A)\zeta_\gamma\zeta_\delta\zeta^*_\lambda\zeta^*_\mu\rho_{(2\gamma+\delta),(2\lambda+\mu)}(\omega,\Omega_p-\omega';\omega,\Omega_p-\omega). \tag{41}$$

As in the general case, we need 16 independent experimental interferograms:

$$G^{(\nu)}(\tau_A) = 2\sum_{k,l=0}^{3} B^{(\nu)*}_l B^{(\nu)}_k\big\{G_{kl} + \rho_{kl}(\tau_a)\big\} \tag{42}$$

with:

$$\rho_{k,l}(\tau_A) = \int d\omega\,\rho_{k,l}(\omega,\Omega_p-\omega)\cos(\omega\tau_A). \tag{43}$$

By using a one-dimensional Fourier transform and performing the same kind of matrix calculations we did for the general case we can recover the matrix we need.

For example, if we consider a polarization-entangled frequency-anticorrelated $|\psi^{(+)}\rangle$ Bell state:

$$|\psi\rangle = \int_{-\infty}^{+\infty} \Phi(\omega)\big\{\hat{a}_{1H}^{\dagger}(\Omega_0+\omega)\hat{a}_{2V}^{\dagger}(\Omega_0-\omega) + \hat{a}_{1V}^{\dagger}(\Omega_0-\omega)\hat{a}_{2H}^{\dagger}(\Omega_0+\omega)\big\}|0\rangle \tag{44}$$

which can also be rewritten as:

$$|\psi\rangle = \int_{-\infty}^{+\infty} \big\{\Phi(\omega)\hat{a}_{1H}^{\dagger}(\Omega_0+\omega)\hat{a}_{2V}^{\dagger}(\Omega_0-\omega) + \Phi(-\omega)\hat{a}_{1V}^{\dagger}(\Omega_0+\omega)\hat{a}_{2H}^{\dagger}(\Omega_0-\omega)\big\}|0\rangle. \tag{45}$$

The two-photon spectral coherence matrix is:

$$R^{(2)}(\omega) = \big|\psi(\omega)\big\rangle\big\langle\psi(\omega')\big|\big|_{\omega=\omega'} = \begin{bmatrix} 0 & 0 & 0 & 0 \\ 0 & |\Phi(\omega)|^2 & \Phi(\omega)\Phi^*(-\omega) & 0 \\ 0 & \Phi^*(\omega)\Phi(\omega) & |\Phi(-\omega)|^2 & 0 \\ 0 & 0 & 0 & 0 \end{bmatrix}. \tag{46}$$

Note that this state exhibit dispersion cancellation, as it appears in the expression $\Phi^*(\omega)\Phi(-\omega)$.

5. Discussion

We introduced a general approach for detailed characterization of the broadband polarization-entangled quantum optical state based on the spectral coherence matrix technique. Several results for single-parameter entangled states described in the literature can be obtained from our general consideration as special cases.

For example, our protocol produces the polarization quantum tomography approach introduced by Kwiat and co-workers [13] when a *monochromatic* two-photon state at frequency Ω_0 is considered:

$$\rho_{(2i+j),(2k+l)}(\Omega,\Omega',\Omega'',\Omega''') = \tilde{\rho}_{(2i+j),(2k+l)}\delta(\Omega-\Omega_0)\delta(\Omega'-\Omega_0)\delta(\Omega''-\Omega_0)\delta(\Omega'''-\Omega_0) \tag{47}$$

when the relation between the measured interferograms and the spectral coherence matrix is:

$$G^{(v)}(\Omega,\Omega') = \sum_{\mu=0}^{15} \Gamma_{v,\mu}\tilde{\rho}_{\mu}\delta(\Omega-\Omega_0)\delta(\Omega'-\Omega_0). \tag{48}$$

The delta-function frequency dependence can be factorized and dropped, thus producing a matrix equation based only on polarization.

In case of a *single photon*, on the other hand, our approach produces known classical spectral coherence matrix. In particular, the density matrix of a broadband single-photon wavepacket, can be expressed as:

$$\rho = \sum_{k,l=0}^{1} \int d\Omega \int d\Omega'\, \rho_{kl}(\Omega,\Omega')|\Omega,k\rangle\langle\Omega',l|. \tag{49}$$

Having just one input spatial mode in such a case, we will need only one tomography device and one detector. The counting rate after integration over time, to account for slow detectors, is therefore:

$$G(\tau) = \int dt\, \mathrm{Tr}\big[\rho E^{(-)}(t)E^{(+)}(t)\big] = 2\sum_{k,l=0}^{1} \zeta_l^*\zeta_k\big\{G_{kl} + \rho_{kl}(\tau)\big\} \tag{50}$$

where:

$$G_{kl} = \int d\omega\, \rho_{kl}(\omega,\omega) \tag{51}$$

and:

$$\rho_{kl}(\tau) = \int d\omega\, \rho_{kl}(\omega,\omega)\cos\omega\tau. \tag{52}$$

The interferograms depend on the elements:

$$R_{ij}^{(1)}(\Omega) = \rho_{ij}(\Omega,\Omega')|_{\Omega'=\Omega} \tag{53}$$

which are the elements of the quantum spectral coherence matrix for the single-photon case. By reducing the dimensionality of the process we defined for the two-photon case we can retrieve the matrix elements $R_{ij}^{(1)}(\Omega)$ from the interferograms.

For example, considering a source emitting the single-photon wavepacket:

$$|\psi\rangle = \int d\omega \left[\epsilon_H(\omega)\hat{a}_H^\dagger(\omega) + \epsilon_V(\omega)\hat{a}_V^\dagger(\omega)\right]|0\rangle \tag{54}$$

we can retrieve the following matrix:

$$\mathbf{R}^{(1)}(\omega) = \boldsymbol{\rho}(\omega,\omega) = \begin{bmatrix} |\epsilon_H(\omega)|^2 & \epsilon_H^*(\omega)\epsilon_V(\omega) \\ \epsilon_H(\omega)\epsilon_V^*(\omega) & |\epsilon_V(\omega)|^2 \end{bmatrix} \tag{55}$$

which corresponds to the classical case (Eq. (13)).

In classical optics, the polarization properties of an optical device can be described by means of a 2-by-2 complex Jones matrix $L(\nu)$. The input and output spectral density matrices $R_0(\nu)$ and $R(\nu)$ are related by the transformation:

$$R(\nu) = L^\dagger(\nu)R_0(\nu)L(\nu). \tag{56}$$

In the same way a similar 4-by-4 complex matrix $T(\nu)$ can be defined for the two-photon polarization-entangled case:

$$R^{(2)}(\nu) = T^\dagger(\nu)R_0^{(2)}(\nu)T(\nu) \tag{57}$$

and can be used to characterize devices or materials that act on the two entangled-photon wavepackets.

However, the more general and informative way to characterize the polarization properties of the material is the Mueller matrix. This is a real 4-by-4 matrix which, for classical light, relates four Stokes parameters of the input beam to the four Stokes parameters of the output beam:

$$\begin{bmatrix} S_0(\nu) \\ S_1(\nu) \\ S_2(\nu) \\ S_3(\nu) \end{bmatrix} = \begin{bmatrix} M_{11} & M_{12} & M_{13} & M_{14} \\ M_{21} & M_{22} & M_{23} & M_{24} \\ M_{31} & M_{32} & M_{33} & M_{34} \\ M_{41} & M_{42} & M_{43} & M_{44} \end{bmatrix} \begin{bmatrix} S_0^{(0)}(\nu) \\ S_1^{(0)}(\nu) \\ S_2^{(0)}(\nu) \\ S_3^{(0)}(\nu) \end{bmatrix}. \tag{58}$$

In the quantum two-photon case the 16 spectral Stokes parameters for the output light will be related to the Stokes parameters of the two-photon input light by means of a 16-by-16 Mueller matrix:

$$\begin{bmatrix} S_0(\nu) \\ S_1(\nu) \\ \cdots \\ S_{15}(\nu) \end{bmatrix} = \begin{bmatrix} M_{0,0} & M_{0,1} & \cdots & M_{0,15} \\ M_{1,0} & M_{1,1} & \cdots & M_{1,15} \\ \cdots & \cdots & \cdots & \cdots \\ M_{15,0} & M_{15,1} & \cdots & M_{15,15} \end{bmatrix} \begin{bmatrix} S_0^{(0)}(\nu) \\ S_1^{(0)}(\nu) \\ \cdots \\ S_{15}^{(0)}(\nu) \end{bmatrix}. \tag{59}$$

6. Conclusions

We have shown that all the quantities normally used to characterize the polarimetric properties of materials and devices in ellipsometry will have a counterpart for two-photon light. One major difference is a significant increase in dimensionality in the quantum case. This increase in dimensionality could be exploited in the field of optical measurement, providing more subtle information about the material system under investigation.

Several approaches have been available in the literature for independent evaluation and characterization of polarization states entangled either in polarization or in frequency. Here we developed a generalized approach providing tools for a detailed characterization of a quantum-optical state that is entangled both in spectrum and in polarization. We accomplished this by generalizing the classical definition of the spectral coherence matrix in order to introduce the two-photon coherence matrix for a broadband two-photon entangled state. We then outlined the experimental procedure for the measurement of its elements and illustrated how it can be used to quantify properties of frequency-polarization entangled states. Moreover, we discussed that such a technique can be used to characterize properties of devices and materials through which such a two-photon entangled state has propagated. We believe that the increased system dimensionality in the quantum case will find applications for optical measurement techniques, particularly in the field of quantum ellipsometry.

Acknowledgements

This work was supported by the National Science Foundation, by the Center for Subsurface Sensing and Imaging Systems (CenSSIS, an NSF Engineering Research Center), by a US Army Research Office (ARO) Multidisciplinary University Research Initiative (MURI), and by IARPA and ARO through grant No. W911NF-07-1-0629. C.B. also acknowledges financial support from Fondazione Cassa di Risparmio di Padova e Rovigo. The authors are grateful to David Simon for helpful discussions.

References

[1] T. Jennewein, C. Simon, G. Weihs, H. Weinfurter, A. Zeilinger, Phys. Rev. Lett. 84 (2000) 4729.
[2] J.L. O'Brien, G.J. Pryde, A.G. White, T.C. Ralph, D. Branning, Nature 426 (2003) 264.
[3] D. Bouwmeester, J.-W. Pan, K. Mattle, M. Eibl, H. Weinfurter, A. Zeilinger, Nature 390 (1997) 575.
[4] J.W. Pan, D. Bouwmeester, H. Weinfurter, A. Zeilinger, Phys. Rev. Lett. 80 (1998) 3891.
[5] J.D. Franson, Phys. Rev. A 45 (1995) 3126.
[6] A.M. Steinberg, P.G. Kwiat, R.Y. Chiao, Phys. Rev. A 45 (1992) 6659.
[7] A.M. Steinberg, P.G. Kwiat, R.Y. Chiao, Phys. Rev. Lett. 68 (1992) 2421.
[8] M.B. Nasr, B.E.A. Saleh, A.V. Sergienko, M.C. Teich, Phys. Rev. Lett. 91 (2003) 083601.
[9] R. Jozsa, D.S. Abrams, J.P. Dowling, C.P. Williams, Phys. Rev. Lett. 85 (2000) 2010.
[10] V. Giovannetti, S. Lloyd, L. Maccone, Nature 412 (2001) 417.
[11] M. Atature, G. Di Giuseppe, M. Shaw, A.V. Sergienko, B.E.A. Saleh, M.C. Teich, Phys. Rev. A 66 (2002) 023822.
[12] J.T. Barreiro, N.K. Langford, N.A. Peters, P.G. Kwiat, Phys. Rev. Lett. 95 (2005) 260501.
[13] D. James, P.G. Kwiat, W.J. Munro, A.G. White, Phys. Rev. A 64 (2001) 052312.
[14] A. Abouraddy, A.V. Sergienko, B.E.A. Saleh, M.C. Teich, Opt. Commun. 201 (2002) 93.
[15] A. Abouraddy, K. Toussaint, A.V. Sergienko, B.E.A. Saleh, M.C. Teich, Opt. Lett. 26 (2001) 1717.
[16] A. Abouraddy, K. Toussaint, A.V. Sergienko, B.E.A. Saleh, M.C. Teich, J. Opt. Soc. Am. B 19 (2002) 656.
[17] K. Toussaint, G. di Giuseppe, K.J. Bycenski, A.V. Sergienko, B.E.A. Saleh, M.C. Teich, Phys. Rev. A 70 (2004) 023801.
[18] D.J.L. Graham, A.S. Parkins, L.R. Watkins, Opt. Express 14 (2006) 7037.
[19] H.-T. Huang, W. Kong, F.L. Terry, Appl. Phys. Lett. 78 (2001) 3983.
[20] R. Barakat, J. Opt. Soc. Am. 53 (1963) 317.
[21] L. Mandel, E. Wolf, Optical Coherence and Quantum Optics, Cambridge Univ. Press, 1995.
[22] P.B. Corkum, N.H. Burnett, M.Y. Ivanov, Opt. Lett. 19 (1994) 1870.
[23] G. Sansone, E. Benedetti, F. Calegari, C. Vozzi, L. Avaldi, R. Flammini, L. Poletto, P. Villoresi, C. Altucci, R. Velotta, S. Stagira, S. De Silvestri, M. Nisoli, Science 314 (2006) 443.
[24] D. Oron, Y. Silberberg, N. Dudovich, D.M. Villenueve, Phys. Rev. A 72 (2006) 063816.
[25] T. Brixner, G. Krampert, T. Pfeifer, R. Selle, G. Gerber, M. Wollenhaupt, O. Graefe, C. Horn, D. Liese, T. Baumert, Phys. Rev. Lett. 92 (2004) 208301.
[26] Y. Silberberg, Nature 430 (2004) 20.
[27] L. Polacheck, D. Oron, Y. Silberberg, Opt. Lett. 31 (2006) 631.
[28] B. Dayan, A. Peer, A. Friesem, A. Silberberg, Phys. Rev. Lett. 93 (2004) 023005.
[29] J. Perina, Coherence of Light, Van Nostrand Reinhold Company, 1971.
[30] N. Wiener, Harmonic analysis and the quantum theory, J. Franklin Inst. 207 (1929) 525.
[31] N. Wiener, Generalized harmonic analysis, Acta Math. 55 (1930) 117.
[32] M.H. Tai, M. Harvit, Appl. Opt. 15 (1976) 15.
[33] W. Wasilewski, P. Wasylczyk, P. Kolenderski, K. Banaszek, C. Radzewicz, Opt. Lett. 31 (2006) 1130.